Experimental analysis of railway track settlement in transition zones

Wang, Haoyu; Markine, Valeri; Liu, Xiangming

DOI
10.1177/0954409717748789

Publication date
2017

Document Version
Final published version

Published in
Institution of Mechanical Engineers. Proceedings. Part F: Journal of Rail and Rapid Transit

Citation (APA)
Wang, H., Markine, V., & Liu, X. (2017). Experimental analysis of railway track settlement in transition zones. *Institution of Mechanical Engineers. Proceedings. Part F: Journal of Rail and Rapid Transit*, *232 (2018)*(6). https://doi.org/10.1177/0954409717748789

Original Article

Institution of MECHANICAL ENGINEERS
Journal of RAIL AND RAPID TRANSIT

Proc IMechE Part F:
J Rail and Rapid Transit
0(0) 1–16

DOI: 10.1177/0954409717748789
journals.sagepub.com/home/pif
SAGE

Experimental analysis of railway track settlement in transition zones

Haoyu Wang, Valeri Markine and Xiangming Liu

Abstract

Transition zones in railway tracks are the locations with considerable changes in the vertical support structures. Due to the differential stiffness and settlement in the open track and the engineering structure resulting in the dynamic amplification of the wheel forces, track settlement is usually observed in the approaching zones. The settlement in transition zones is detrimental to the track components and passenger comfort. This paper presents the results of the experimental analysis performed in three transition zones which were in various conditions. The dynamic displacements of rails due to passing trains were measured at multiple points (dynamic profile) in the approaching zones. The device employed is a contactless mobile device for measuring displacements, which is based on the digital image correlation technique. Because the operational parameters of the digital image correlation-based devices are important for measurement accuracy, prior to the in situ measurements, this device was tested in a laboratory to study the influence of the operational parameters, including the elevation/heading angles, the focal length of the cameras, and the measuring distance. After determining the optimal operational parameters for the railway field, multiple-point measurements were performed in the transition zones. The length of the approaching zone was studied first. Also, the dynamic profiles of the embankment–bridge and bridge–embankment transitions were analysed. Finally, by comparing the multiple-point displacements in the approaching zones in different conditions, it was found that the dynamic profile of the rail displacements has a good correlation with the track condition in the transition zone. The results are presented and discussed.

Keywords

Railway, transition zone, measurement, digital image correlation

Date received: 6 April 2017; accepted: 16 November 2017

Introduction

Transition zones in a railway track network are locations with considerable change in the supporting structures. Typically, they are located near engineering structures, such as bridges, culverts and tunnels. A typical track transition zone is shown in Figure 1, wherein an embankment is connected with a culvert.

In such locations, the vertical stiffness of the track support abruptly changes, resulting in amplification of the dynamic forces acting on the track, which ultimately leads to accelerated deterioration of the vertical track geometry.[1–3] In addition, since the engineering structures always settle much slower than the embankment, the differential settlement between the engineering structure (e.g. bridge) and open track always occurs. Such initial settlement contributes significantly to the amplification of the wheel forces and ultimately to the deterioration of the track geometry in the transition zone.[4,5] Therefore, maintenance of the track geometry in the transition zones requires substantial efforts. For example, in the Netherlands, the track maintenance in the transition zones is performed up to four to eight times more often than on the open track.[6,7] In the US, $200 million is spent annually to maintain the transition zones, while in Europe about 97 million is spent.[8,9]

The ballast track in the transition zones can be divided into two parts (Figure 2): the open track that is relatively far from the engineering structure and therefore unaffected by the presence of the engineering structure and the approaching zone which is located close to the engineering structure and suffers from the settlement.[2,5,10,11] The settlement in the approaching zone, showed as a dip in Figure 2(b), typically appears shortly after installation/renewal of the track. This phenomenon has been confirmed by a survey of the performance of track transition zones, which revealed that 51% of the studied transition

Delft University of Technology, Delft, The Netherlands

Corresponding author:
Haoyu Wang, Stevinweg 1, 2628CN, Delft, The Netherlands.
Email: H.Wang-1@tudelft.nl

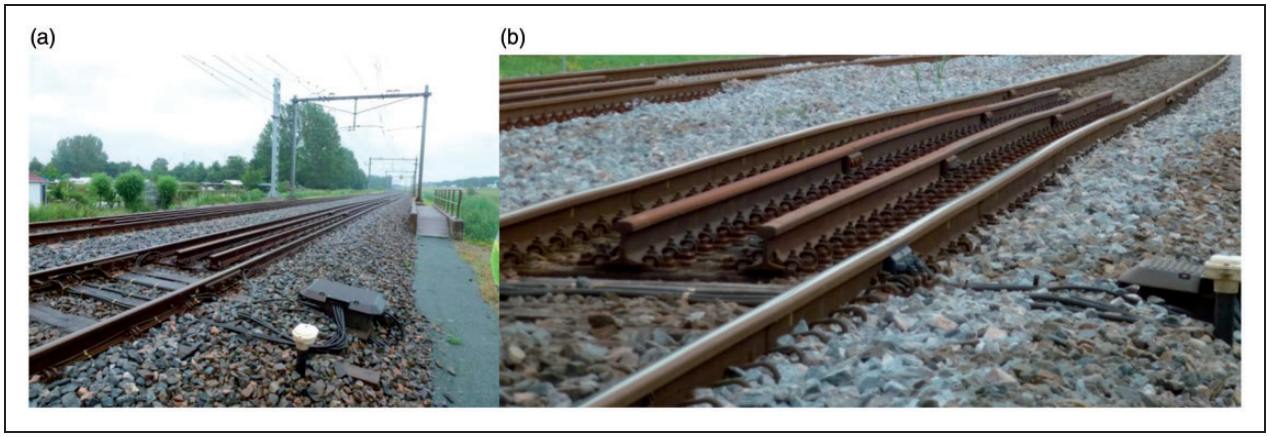

Figure 1. A typical track transition zone: (a) global view and (b) close-up view.

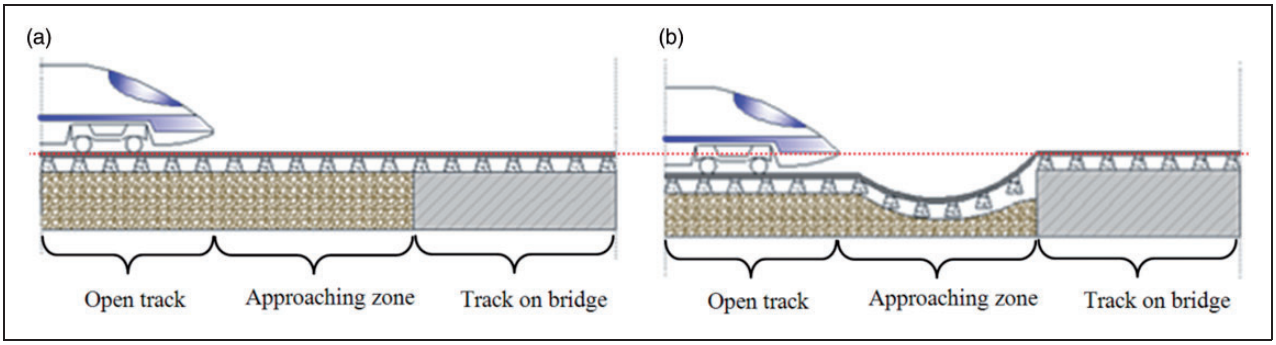

Figure 2. Schematic diagram of the differential settlement in the transition zone: (a) immediately after construction or maintenance (no settlement) and (b) after a few months of operation.

zones had experienced such a settlement.[3] The dip also appears in the transition zone between the embankment and the level crossing.[12]

Theoretically, such a significant irregularity in the track geometry may trigger considerable wheel–rail interaction forces, which may result in damage to the track components, affect the passenger comfort, and even lead to a train derailment. Ultimately, it may raise the need for additional maintenance and may increase the life cycle costs. However, the length of the approaching zone and the magnitude of the settlement (the profile of the settlement) usually are not clearly defined. Therefore, the maintenance of the track in the transition zone is difficult to plan and to perform timely.

The field measurements and analysis of the transition zone behaviour are somewhat lacking or even scarce.[2] Gallage et al.[13] stated that the track degradation in the transition zones is far from being solved because the mechanism of applied countermeasures is not entirely understood. Paixao et al.[14] also pointed out that despite the efforts undertaken to minimise the track transition zone problems, the transition zones continue to exhibit poor performance and a considerable amount of maintenance effort was still spent at these locations. Similarly, such track transition zones experiencing severe settlements have been observed by the authors during this study.

In some studies, the measurements in the transition zones performed at one point in the approaching zone are later compared with one point measured in the open track and one point measured on the bridge, such as in Zuada Coelho,[2] Stark and Wilk[5] and Li and Davis.[10] In this way, the location and the amplitude of the dynamic profile of the dip (Figure 2(b)) are not clear. A better method is to measure the displacement of sleepers at multiple locations simultaneously in the approaching zone, such as in Le Pen et al.[12] and Coelho et al.[15]

Similar to the idea of multiple-point measurements in Le Pen et al.[12] and Coelho et al.,[15] this paper presents the results of the experimental study performed on three transition zones. The dynamic displacements of the rails in this study are measured simultaneously at multiple points (up to eight points, with a minimal spacing of 0.6 m) in the approaching zone so that the dynamic profile of the track displacements can be obtained. The measurement device used in this study is a contactless mobile device for measuring displacements based on the digital image correlation (DIC) principle. The measuring method was first presented in Wang et al.[16] and later in Markine et al.[17]

By studying the dynamic responses in the transition zones, the following aspects are discussed in this paper:

1. The length of the approaching zone (that is affected by the settlement);
2. The dynamic profiles of the rail displacement in the embankment–bridge and the bridge–embankment transitions;
3. The dynamic profiles of the transition zones in various conditions.

A brief overview of the measurement techniques used in the transition zones is given in the next section. Since the operational parameters of the DIC-based devices are important for measurement accuracy and the device used here had not been applied for railway measurements, it was tested in the laboratory first. The sensitivity of the operational parameters, including the measuring angle, the distance and the focal length of the lens, was analysed in the 'DIC-based measurement devices' section. After that, the measurements of the dynamic displacement at multiple points on the rails in the approaching zones were performed and the dynamic behaviour of the track was analysed as presented in the 'Field measurements in transition zones' section and discussed in the 'Discussion' section. Finally, the findings and conclusions are summarised in the 'Conclusion' section.

Measurement techniques in transition zones

The vertical rail displacements in the transition zones discussed in the literature can be divided into two categories, namely the permanent displacements and the transient ones. The permanent displacement, also named settlement, is the absolute static rail displacement referring to the original position without loading, while the transient displacement is the relative rail displacement during train passage with respect to the unloaded position. When the contact between sleepers and ballast is in good condition, such as in the open track, the transient displacement of the rail should remain constant, while the permanent displacement may grow slowly. However, in the approaching zones, the contact status between sleepers and ballast is often poor, which is presented by a void in ballast under sleepers and also called hanging sleeper.[18,19] Due to the void, the hanging sleepers can move with less constraint during the passage of trains. The stress in ballast adjacent to the hanging sleeper is increased and later leads to track degradation.[5] Therefore, the transient displacements of the track can indicate the track degradation. Usually, the higher the transient displacements in the transition are, the worse the condition of the transition zone is. The number of the experimental studies of transition zones is rather limited as compared to the studies of other sections of track. An overview of the experimental studies and the measurement techniques used therein available in the literature is given below.

Li and Davis[10] studied the plain transition zones (the transition zone without countermeasures), wherein the permanent settlement of the track was measured using the *optical level*. It was found that the settlement in the open tracks was larger than the settlement on the bridges, but smaller than those in the approaching zones. Later, Hyslip et al.[8] studied the track geometry data of two transition zones. The data were obtained by automated track geometry *measurement vehicles* for a period of three years. It was also reported that the rail at the bridge approaching zone settled after tamping and resulted in a dip in the track reoccurring near the bridge, and the reason for the settlement was that the tamping maintenance process loses effectiveness near the fixed structure. A recent measurement was conducted in Stark and Wilk,[5] who used linear variable differential transformers (LVDTs) to measure the permanent settlement and transient displacements in the two transition zones. It was found that the permanent settlements in the approaching zone were much bigger than those in the open track only after a half-year of operation.

A transition zone using approaching slab has been experimentally studied in Zuada Coelho[2] and Coelho et al.,[15] wherein the transition zone used a 4 m reinforced concrete slab on each side of the culvert. The concrete slab was laid under the ballast layer with one end hinged at the culvert and the other end free in the embankment. *Geophone* was used to measure both the permanent and the transient sleeper displacement during train passages. It was also found that the biggest transient displacements of the sleepers were in the approaching zones, while the displacements on the culvert were the smallest.

As for the high-speed tracks, a laser-based monitoring system, position sensitive detector (PSD), was used to measure the transient displacements of rails in a transition zone in the Portuguese high-speed railway (220 km/h).[20] Later, LVDTs and PSDs were used to measure the transient displacements of rails in a transition zone in the Spanish high-speed railway (220 km/h). Since the transition zones were well constructed with the reinforce backfill, no differential settlements were found in the approaching zones.[21,22] However, since the design and maintenance of the transition zones in the high-speed tracks are different from those in the normal-speed tracks, these two studies are not considered here.

In the transition zone between the embankment and the level crossing, *geophones, DIC-based devices* were used to measure the transient displacement of multiple sleepers in the approaching zone.[12] A dip (dynamic profile) was found, located from 2.52 to 7.83 m and centred at 5.15 m.

All the available measurement results in track transition zones are summarised in Table 1.

Based on this review (Table 1), the following conclusions can be made:

1. The displacements in the approaching zones are the largest, while the displacements on the bridge are the smallest ones, in both permanent and transient measurements performed on the normal-speed tracks.
2. The field measurements in transition zones in a railway track are relatively insufficient in number. Also, the measurements did not cover transitions in different conditions.
3. The behaviour of transition zones is complex and difficult to predict. Also, this behaviour depends on the design of the transition zones, i.e. with or without various countermeasures. Even for the transition zones of the same type, the behaviour may vary, depending on the geotechnical conditions and train operation. For example, in Nicks[3] one half of the studied transition zones suffered from severe settlements, while the other half not. Therefore, it is necessary to propose an assessment method, which can easily evaluate the quality of transition zones.
4. Some countermeasures did not improve the performance of transition zones. For example, there was no reduction of the permanent settlement in the transition zones achieved by HMA, cement and geocell as compared to the transition zone without countermeasures (e.g. Li and Davis[10]). Using the approach slab has an even negative effect on the settlement reduction in transition zones.[2]
5. In most mentioned measurements, only one point was measured in each zone, i.e. open track, the approaching zone and the bridge. However, using only one point is difficult to capture the location with the largest displacement. Also, the length of the affected approaching zone is not known. Coelho et al.[15] measured five sleepers in the approaching zone. However, due to the rotation of the approaching slab, the dynamic profile was different from that of the plain transition zones. Also, in the measurement of the transition zone of the level crossing,[12] seven sleepers in the approaching zone were measured. Due to the structural difference of the level crossing, the dynamic profile was also different. Although the transition structures are different, the method that measures at multiple points of the approaching zone was successfully proved to provide more insights of the track behaviour than the one-point measurement.

The paper presents the detailed experimental study of three transition zones in various conditions. The dynamic profiles of transition zones were measured simultaneously in several points instead of one point, using a DIC-based device. The results of the

Table 1. Summary of the results of measurement in track transition zones.

	Vertical displacement sleepers/track (mm)					
Measured displacements	Open track	Approaching zone	Bridge	Countermeasures	Measuring equipment	Reference(s)
Permanent	29.2	35.3	16.2	– (Plain)	Optical level	Li and Davis[10]
	45.4	47.3	19.1	Hot mix asphalt (HMA)		
	35.6	40.2	18.3	Cement		
	39.4	43.4	15.8	Geocell		
	24.9	16.4	0.3	Concrete approaching slab	Geophone, high-speed camera	Zuada Coelho[2] and Coelho et al.[15]
	2.0	3.6	–	– (Plain)	LVDT	Stark and Wilk[5]
	0.5	7.2	–	– (Plain)		
Transient	1.2	6.8	0.8	Concrete approaching slab	Geophone, high-speed camera	Zuada Coelho[2] and Coelho et al.[15]
	0.8	11.2	0.3			Zuada Coelho[2] and Coelho et al.[15]
	0.4	1.7	–	– (Plain)	LVDT	Stark and Wilk[5]
	0.8	5.2	–	–	Geophone, DIC	Le Pen et al.[12a]
	0.6	0.5	0.4	Backfill	PSD	Pinto et al.[20b]
	0.8	0.5	0.5	Backfill	LVDT, PSD	Paixão et al.[21,22b]

DIC: digital image correlation; LVDT: linear variable differential transformer; PSD: position sensitive detector.
[a]The measurements for the transition zone of a level crossing instead of a bridge.
[b]The measurements are for the high-speed lines, while the rest are for normal-speed lines.

field measurements using the DIC-based devices in railway are described in the following section.

DIC-based measurement devices

In this section, the measurement device used here, which is based on the DIC, is presented. The DIC-based devices have been widely used in civil engineering mainly to measure the plastic deformation of concrete bridges[23,24] or the strain of material.[25–27] However, a relatively small number of papers reported that DIC-based devices were used in the railway field, where the displacements at higher frequency are generated. The applications of the DIC-based devices in railway field are reviewed first. After that, several sensitive operational parameters of the DIC-based device were tested, since it has never been used for railway purposes before.

Application of DIC-based devices in railways

DIC is an optical method, which uses tracking and image registration techniques for accurate measurements in images. A reference image is captured before displacement and a series of pictures are taken subsequently during the movement. The images are analysed using a numerical matching technique to identify the most similar patterns in the subsequent images, which is based on the assumptions that the pattern is approximately constant between successive images and that the local textural information is unique. The matching algorithm compares the image subsets in the reference image with the image subsets in the current image.[28] Matching criteria are available such as in Giachetti[29] and Tong.[30] The method combines continuous recording of horizontal and vertical displacements with no contact with the measuring targets, excluding any interference between the measured surface and the measuring device.[24,26,31] It often consists of high-resolution digital cameras which record the displacement of targets and post-processors which analyse the changes in the images.

Bowness et al.[32] successfully employed a DIC-based device to measure the complex dynamic deflection histories of sleepers at three locations during train passages, which was validated by geophones. Accurate measurement results were achieved up to 100 km/h of the train speed by using a 30 fps camera. However, the authors pointed out that only one sleeper or location could be monitored at a time. The similar comparison between the DIC-based device and geophones can also be found in Priest et al.[33] and Priest and Powrie.[34] In addition, the ground vibration has a small influence on the camera at a distance of 6 m from the rail.[32] A recent study discussing the ground vibration could be found in Wheeler et al.[35]

The measured train speed was raised to 180 km/h in Ribeiro et al.,[36] using a camera up to 500 fps, in the measurements of railway bridges. The measurement results were validated by LVDTs and the obtained precision was below 0.1 mm for the distance of 15 m. The displacements of rail were measured by a DIC-based device in Murray et al.[37] By using four synchronised cameras, multiple locations along the track were measured. The cameras were 100 fps and they were positioned at a distance of 10 m. The rail strains measured by DIC-based devices were compared to finite element simulation results, and a good correlation is achieved again.[38]

Le Pen et al.[12] measured the displacements of sleepers along the transition zone between the embankment and a level crossing using DIC devices. The train speed was around 112 km/h. The measurement results at multiple locations had a good correlation with geophones. In most cases, the measurement results of DIC have better quality than those of geophones.

Compared to the traditional measurement methods used in railway fields, such as LVDT and geophones, the DIC-based devices have some advantages.[32,33,37] The major advantage of the DIC-based devices is that they can perform measurements from a distance. Therefore, the measurements can be performed in a safe zone of a railway track, for example staying at a distance further than 3.25 m from the track. The zone within 3.25 m is a dangerous zone according to the Dutch railway safety regulations. In addition, the installation of DIC-based devices is less time consuming. The traditional contact measuring equipment requires at least one maintenance window (track possession) to be installed on the track (e.g. attaching sensors to the rails) and another window to be removed. However, most of the installation work of the DIC-based devices, including setting cameras and computers, can be conducted outside of the track that does not require the possession time. Moreover, the DIC-based devices can obtain the measurement data off-line, i.e. the recorded videos can be processed later in the office. Besides, DIC-based devices can measure the absolute displacements instead of the relative displacement.

Since the possession time of tracks is expensive and the access to the track is increasingly difficult, DIC-based devices have become very attractive in the monitoring of railway tracks. In this study, a DIC-based device is applied to measure the rail displacements at multi-points in the transition zones. Because the operational parameters of the DIC-based devices, which may be limited in the railway field operation, are important to accuracy, the device was tested in the laboratory to study the sensitivity of the key parameters. The main limitations of the DIC-based devices in practical operation are as follows:

1. The elevation and heading angle of cameras to targets should be small enough. Ideally, the cameras should be perpendicular to the displacement

plane of the measured targets. However, in most cases, cameras have to face the measured targets with the elevation and/or heading angle, due to the constraint of the track field. For example, the two inner rails of a double track railway are always blocked by the outer rails.

2. There is a conflict between the field of view and the resolution of cameras. A larger field of view and a higher resolution of the camera are both desirable but cannot be achieved at the same time. On the one hand, a larger field of view can cover more sleepers; on the other hand, the larger field of view reduces the resolution of the camera, which affects the measurement accuracy. To study the relationship between the measurement accuracy and operational parameters, a series of experiments were performed in the railway laboratory of Delft University of Technology, the Netherlands.

Laboratory tests of the operational parameters

The operational parameters to test are the elevation and heading angle, the measuring distance and the focal length. The DIC-based device used here consists of cameras (up to 400 fps), lenses of various focal lengths and a processing system, as shown in Figure 3. The system is called video gauge system and provided by Imetrum.

In the laboratory tests, the DIC-based device was used to measure the motion of the actuator of a hydraulic press machine, which is the periodic vertical motion with the frequency of 0.1 Hz and the peak–peak amplitude of 10 mm. The tested operational parameters are shown in Figure 4. The tested values of the operational parameters of the device are shown in Table 2. The reference combination of the parameters is 0° elevation angle, 0° heading angle, 7.5 m measuring distance and 75 mm lens (the values in bold in Table 2). During the test, the values of only one parameter were changed, while the other parameters have the reference values. The results of the testing details are presented in Markine et al.[17] The influence of the operational parameters on the measurement accuracy is shown in Figure 5.

From Figure 5, it can be seen that the average error and the standard deviation in all the tests are less than 5% and 5‰, respectively. This confirms the feasibility of the DIC-based device for railway engineering

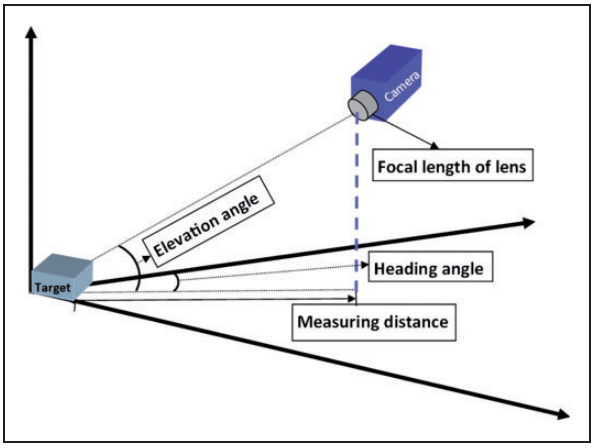

Figure 4. Illustration of the operational parameters.

Table 2. Tested value of the operational parameters.

Parameters	Values
Elevation angle (°)	**0**, 2.5, 5, 7.5, 10
Heading angle (°)	**0**, 5, 15, 30, 45
Measuring distance (m)	2.5, 5.0, **7.5**
Focal length of lens (mm)	16, 25, 50, **75**

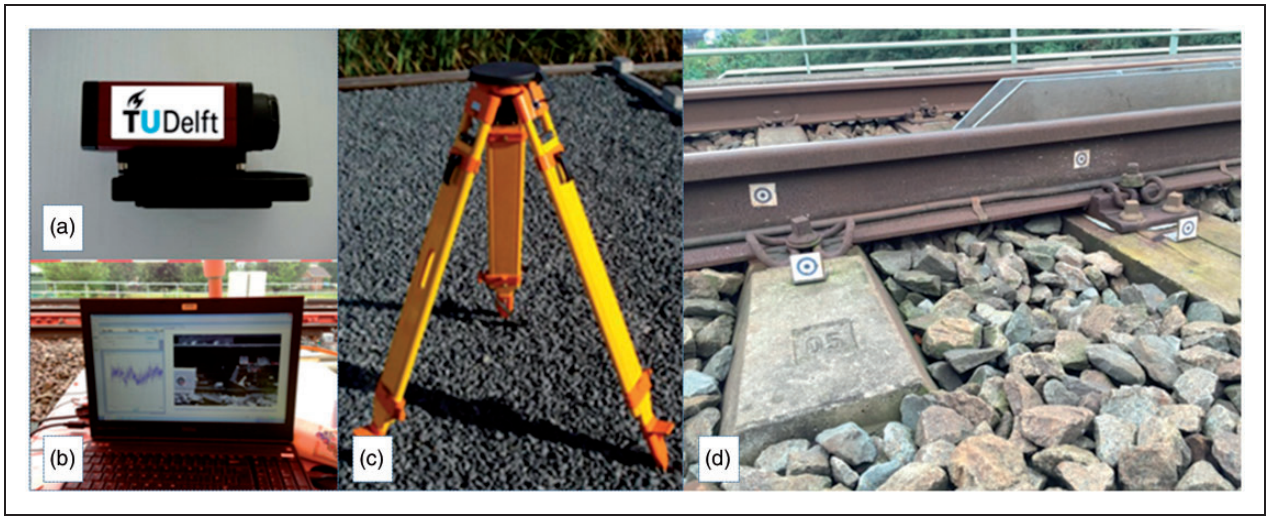

Figure 3. Components of the DIC-based device: (a) a high-speed camera, (b) the processing system, (c) a tripod and (d) targets.

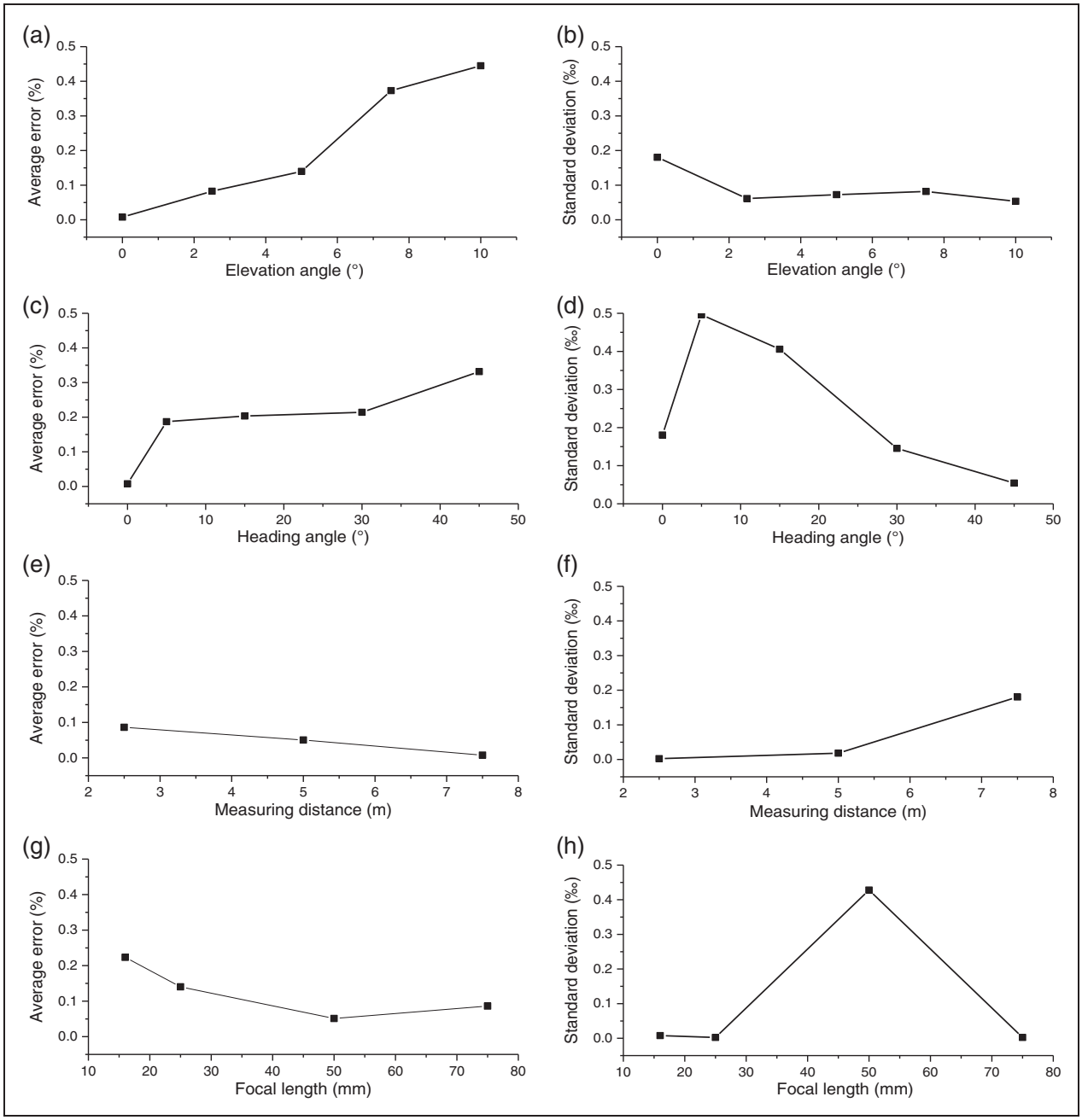

Figure 5. Effect of the elevation angle: average error (a) and standard deviation (b), effect of the heading angle: average error (c) and standard deviation (d), effect of measuring distances: average error (e) and standard deviation (f) and the effect of focal length: average error (g) and standard deviation (h).

applications, as in Bowness et al.,[32] Priest et al.,[33] Ribeiro et al.[36] and Iryani et al.[38]

Although both the elevation and the heading angles can generate the average error, the average error is more sensitive to the elevation angle rather than the heading angle. As it can be seen from Figure 5(a) and (b), the average error reaches 4.5% when the elevation angle is 10°, while the average error is only 3.3% when the heading angle is already 45°. This is logical since the target is moving in the vertical direction. Even though the angles are inevitable due to the field restrictions, the heading angle should be constrained to 30° and the elevation angle should be constrained to 10° with respect to the accuracy of measurements.

On the contrary to the angles, the average error introduced by the measuring distance is relatively small, as shown in Figure 5(e). To increase the field of view (to measure as many sleepers as possible) while not reducing the accuracy, a long measuring distance, for instance 7.5 m, is recommended. Measuring on a long distance has a clear advantage, since the effect on the ground vibrations due to the passing trains will be reduced. The measuring distance of 7.5 m is also beyond the so-called dangerous zone in the Netherlands, wherein the human presence is not

allowed if the track is in operation. The focal length of 50 mm for the reference distance (7.5 m) generates the smallest average error (Figure 5) and it is therefore recommended.

Finally, the proposed operational parameters are listed in Table 3. Note that the elevation angle is smaller than 10° when the distance is 7.5 m and the height difference between the camera and the rail is 1.3 m.

With a better understanding of the measuring device, the field measurements in the transition zones were conducted, which are presented in the following section.

Field measurements in transition zones

The measurements of the transition zones using the DIC-based device are analysed in this section. The purposes of the measurements are as follows:

1. to determine the length of the approaching zone in transition zones;
2. to explore the difference of the dynamic profiles of the embankment–bridge and bridge–embankment transitions;
3. to study the relationship between the dynamic profile and the health condition of transition zones.

Field introduction

Three transition zones were measured using the DIC-based device, which are named Transitions A, B and C as shown in Figure 6. In Transitions A and B, the embedded rail system is used on the bridges, while the ballast track with concrete sleepers is used on the embankment, as shown in Figure 6(a) and (c), respectively. According to the maintenance history, Transition A was in poor condition while Transition B in healthy condition. Therefore, larger dynamic displacements were expected in the approaching zone than in the open track in Transition A. In Transition C, the ballast was used above the bridge and the performance was also in poor condition as shown in Figure 6(e).

The layout of the measurements in the three transition zones is given in Figure 7. The first sleeper was located at 0.3 m from the abutment of the bridge and the sleeper spacing was 0.6 m. The measured locations are indicated by the red circles. During the measurement of Transition A, two synchronised cameras were used. One measured the track close to the bridge, from 0 to 2.4 m; the other measured the track further, from 4.2 to 6 m. The rail at 60.3 m was measured apart since it is too far from the bridge. In total, seven train passages were measured in the approaching zone and eleven train passages were measured in the open track. The measuring frequency was 78 Hz. Similarly, the measuring frequency in Transition B was 78 Hz. The embankment–bridge and bridge–embankment transition were measured separately. Forty-two train passages were measured in the embankment–bridge transition and were measured in the bridge–embankment transition. In the measurement of Transition C, the measuring frequency was 31 Hz and four train passages were recorded.

Table 3. Suggested values of the operational parameters.

Parameter	Suggested value
Elevation angle (°)	<10
Heading angle (°)	<30
Measuring distance (m)	7.5
Focal length (mm)	50

The passing trains are the Dutch passenger trains. Their geometrical parameters are shown in Figure 8.[2] Their velocities are between 80 and 140 km/h, while the axle loads (empty train) are around 16 t. During the measurement, the velocities were around 100 km/h. The setting of the DIC-based device was the same as proposed in Table 3.

Using the measurement data in Transition A, the length of the approaching zone is analysed. The rail displacements measured in the open track (at 60.3 m from the bridge) are compared with the rail displacements closer to the bridge. Since the performance of Transition A was in poor condition, larger dynamic displacements are expected in the approaching zone than in the open track. Moreover, using the measurement results in Transition B, the dynamic profiles of the embankment–bridge and bridge–embankment transitions are analysed. In addition, compared with the measurement results of the embankment–bridge transitions in Transitions A, B and C, the relationship between the dynamic profile and the performance is studied.

Length of the approaching zone

The measured examples of the displacements of the rail at −1.5, −4.5 and −60.3 m (the open track) in Transition A are shown in Figure 9. Note that the number of the distance is calculated from the end of the abutment. For convenience, a negative sign is used to indicate the left side of the bridge (the embankment–bridge transition) while a positive sign is used to indicate the right side (the bridge–embankment transition).

As can be seen in Figure 9, the peaks in the time history curves correspond to the passage of each wheelset. In the frequency domain, the peaks match very well with the frequencies due to the characteristic length of the train. Taking the displacement of Rail −0.9 m (Figure 9(b)) for example, when the velocity of the trains is around 100 km/h, the first characteristic frequency is 1.38 Hz that corresponds to the bogie distance of 20 m (Figure 8); the second characteristic frequency is 4.00 Hz that corresponds to the distance

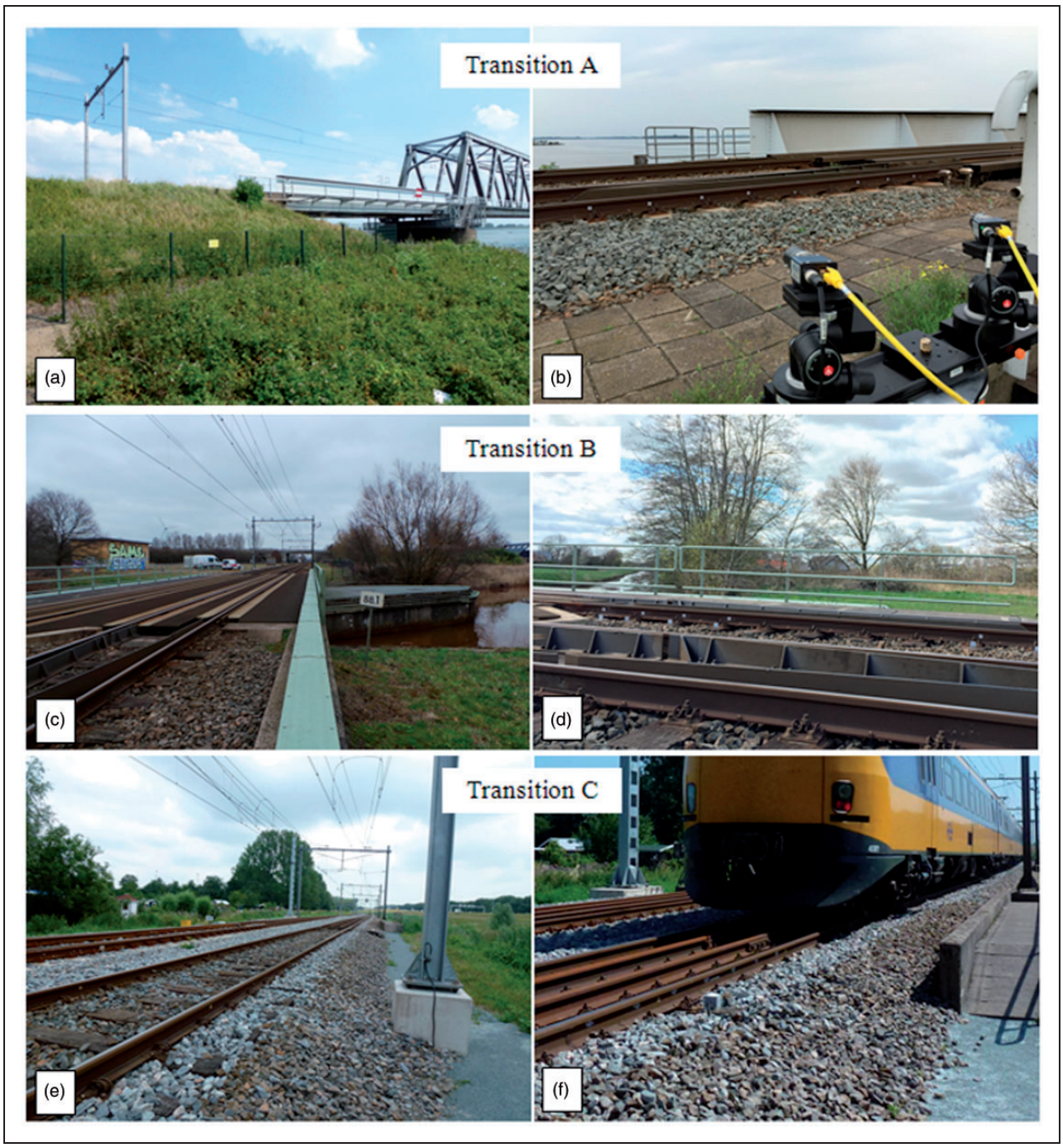

Figure 6. Photos of Transitions A, B and C: overall photos (left) and partial photos of the targets on the rail (right).

between two bogies of the neighbouring vehicles of 7 m; the characteristic frequencies of 9.38 and 10.75 Hz correspond to the wheel distance in the bogies of 2.8 and 2.5 m, respectively. These characteristic frequencies can also be found in the measurements in other locations (Figure 9(d), (f) and (h)). This shows that the results measured by the DIC-based device are correct.

Comparing the displacements measured in the three locations (Figure 9), it can be concluded that the approaching zone in this transition is within 4.5 m from the abutment of the bridge, since the displacements at −4.5 m (Figure 9(e)) are similar to the ones at the open track (Figure 9(g)), and much smaller than the displacements at −0.9 and −1.5 m (Figure 9(a) and (c)).

In the measurements shown in Figure 9, the maximal displacements at 60.3, 4.5, 1.5 and 0.9 m are 0.88, 0.82, 5.19 and 5.55 mm, respectively. In the same way, the maximal displacements in other passages were collected. The average values of the maximal displacements of at multiple locations can be considered as the dynamic profile of Transition A as shown in Figure 10.

From Figure 10, it can be seen that the approaching zone is most likely located within 4.5 m from the

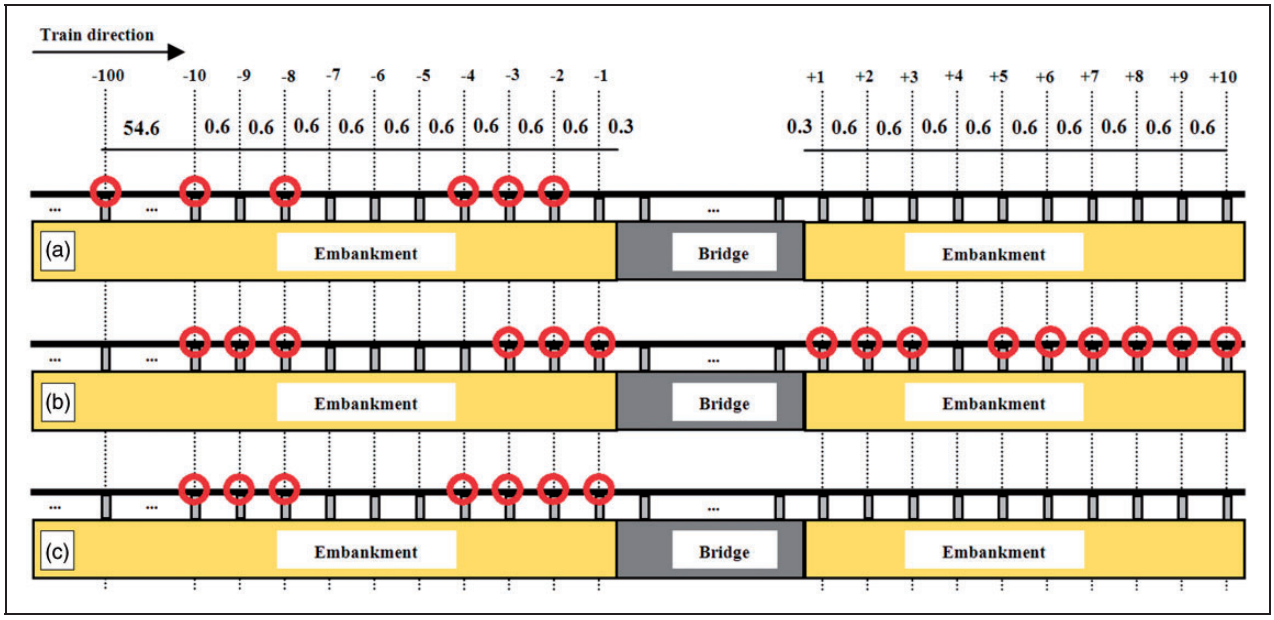

Figure 7. Schematic plan of measurements.

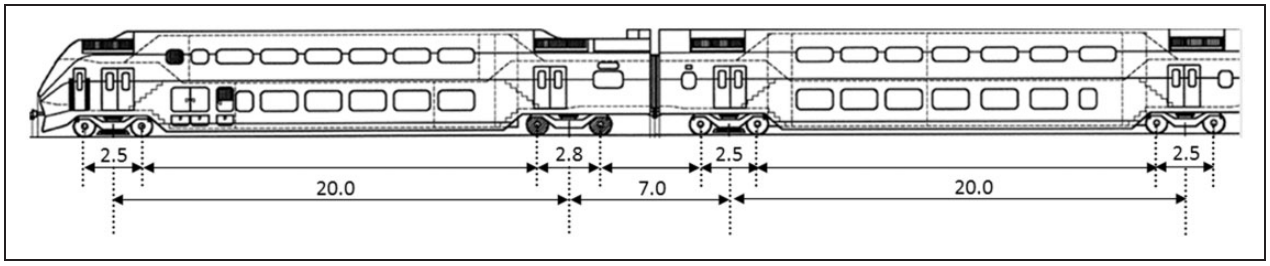

Figure 8. Vehicle configuration.

bridge. Since the condition of the Transition A was considered as poor, the track settlement in the approaching zone is naturally larger than in the transition zone of good condition. Therefore, 4.5 m can be considered as the upper limit for the length of the approaching zone for this type of transition zone. Note that since the length of the approaching zone depends on its engineering structure and the local subgrade property, it is only valid for similar transition zones. To validate this assumption and to study the approaching zone, the rail displacements were also measured in another two approaching zones. The results of these measurements are discussed in the next section.

Dynamic profiles of the embankment–bridge and bridge–embankment transitions

The measured examples of the rail displacements in both the embankment–bridge and the bridge–embankment transitions in Transition B are shown in Figure 11. The rail displacements measured at the symmetric locations of the bridge are compared.

As can be seen in Figure 11, the peaks at the symmetric locations in the embankment–bridge and the bridge–embankment transition zones are generally similar, except that at ±0.9 and ±1.5 m the rail displacements on embankment–bridge are larger. The largest difference is around 30%, which can be found in Figure 11(b), where the maximal displacement at −0.9 m is 2.69 mm while that at +0.9 m is 2.37 mm. It is in agreement with the theoretical analysis in Kerr and Moroney[1] and numerical simulation in Wang et al.,[4] wherein the dynamic behaviour of the train in the two types of transition zones is different. It is a remarkable fact that Transition B is in healthy condition. For transition zones in poor condition, the simulation may be different.

Figure 11 also shows that the rail displacements at the close locations (±0.3, ±0.9 and ±1.5 m) are much larger than those at the relative distant locations (±4.5, ±5.1 and ±5.7 m), which is in agreement with Transition A. The dynamic profile of Transition B is described in Figure 12.

As seen in Figure 12, the dynamic profiles of the two types of transitions are both increased close to the bridge. The rail displacement in the embankment–bridge transition gradually decreases from 0.3 to 4.5 m. Differently, the largest rail displacement in the bridge–embankment transition zones appears at

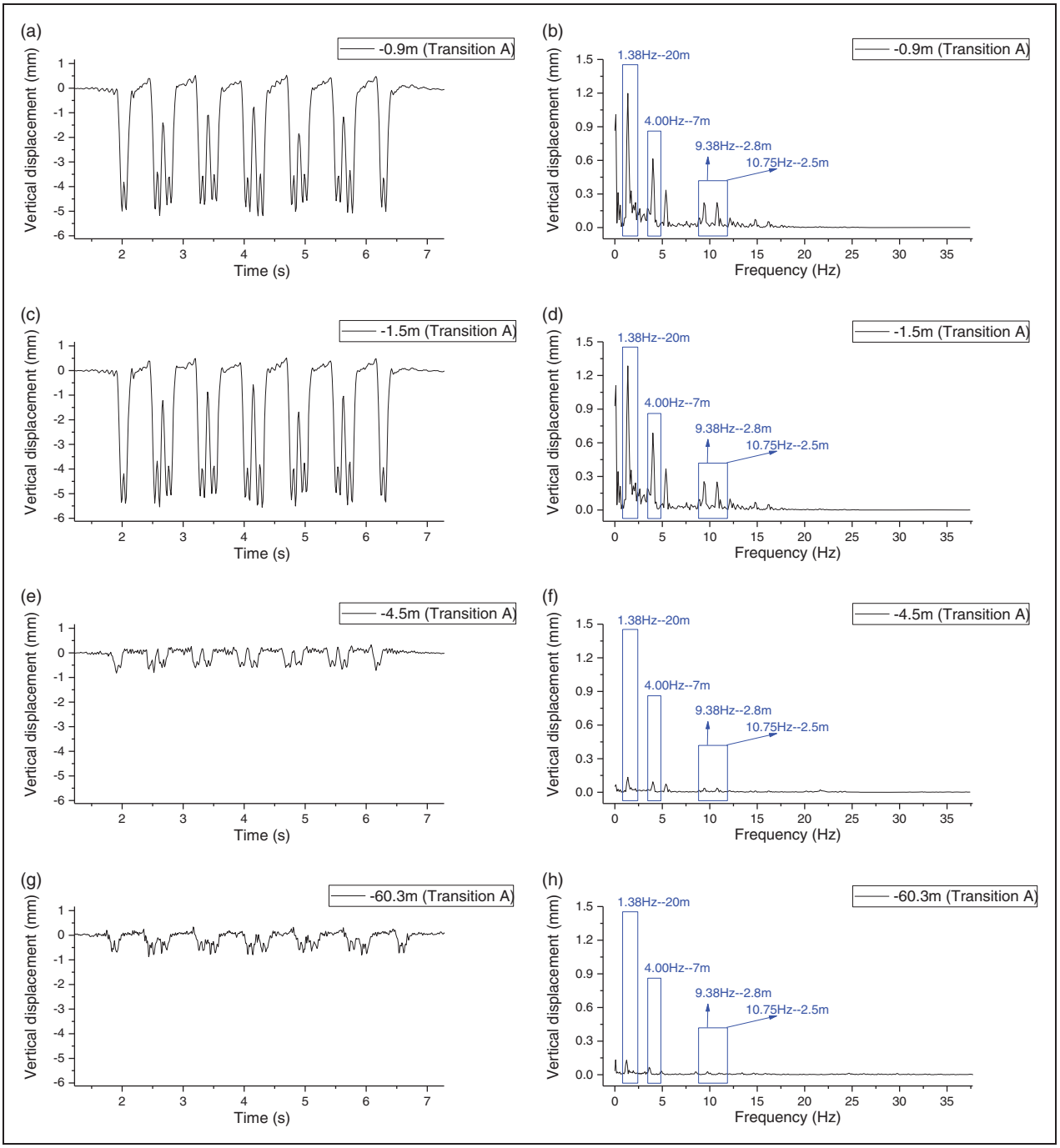

Figure 9. Rail vertical displacements at four locations of Transition A in the time domain (a), (c), (e) and (g) and in the frequency domain (b), (d), (f) and (h).

0.9 m instead of the 0.3 m (the closed one). This is discussed later.

Dynamic profiles of transitions in various conditions

The example of the rail displacements measured at −1.5 and −4.5 m in Transitions A, B and C is shown in Figure 13. The maximal displacements corresponding to the passing bogies are listed in Table 4.

Comparing the results obtained in Transition B and Transitions A and C, it can be seen that the rail displacements at −4.5 mm are similar as shown in Figure 13(c), which are 1.06, 0.63 and 1.06 mm, respectively (Table 4). It is reasonable, since the rail displacements at −4.5 m are close to the displacements in the open tracks, and the open tracks in the three transition zones are similar. The rail displacements at −1.5 m in Transitions A, B and C are considerably different, which are 5.27, 2.27 and 4.86 mm, respectively (Table 4). This means that the void at −1.5 m in Transitions A and C is larger than in Transition B. Hanging sleepers are expected in such

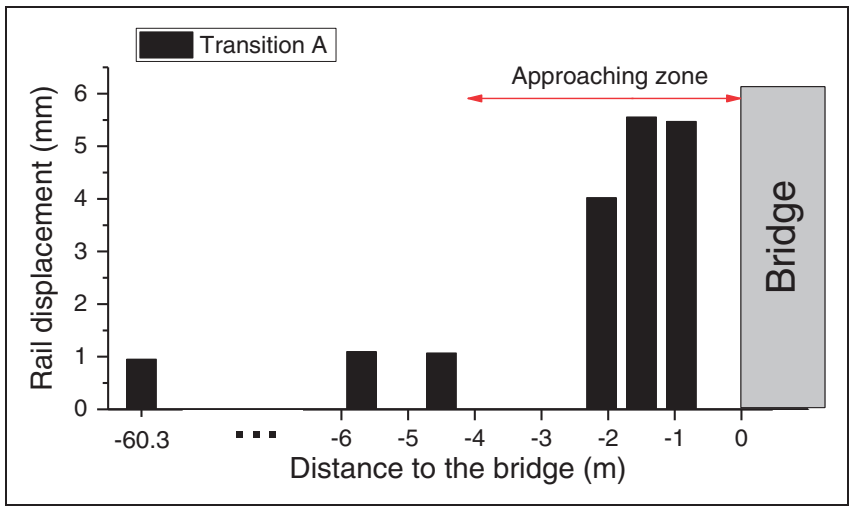

Figure 10. Statistics of the vertical rail displacements at all measured points of Transition A.

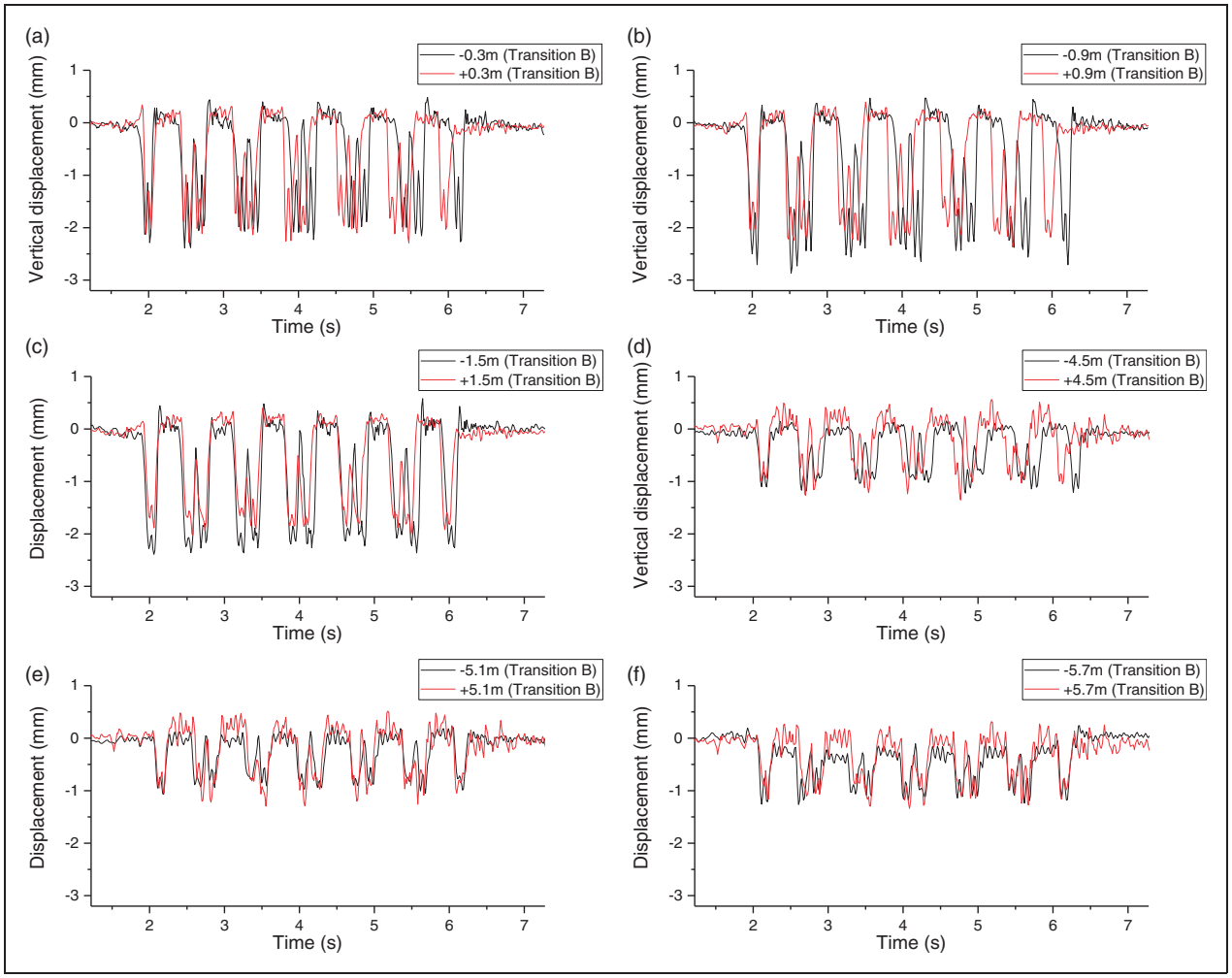

Figure 11. Rail vertical displacements in the embankment–bridge and the bridge–embankment transitions of Transition B.

locations. Therefore, the tracks in Transition A and C are in worse condition than in Transition B, which is in agreement with the health condition known from the maintenance history. Based on the measurement results, the dynamic profiles of Transitions A, B and C were obtained, which are compared in Figure 14.

As can be seen in Figure 14, the rail displacements are sharply increased in the approaching zones

(0.0–4.5 m) in all transition zones, in comparison to the rail displacements in 0.3–1.5 and 4.5–5.7 m zones. The larger rail displacements confirm the 'dip' often reported in the transition zones (e.g. Nicks[3]). The high displacements of rail indicate that the sleepers are in poor supporting condition, which leads to a significant redistribution of the wheel load.[4,5]

The increase of the rail displacements near the abutment (0.3–1.5 m) in these transitions can be caused by the dynamic behaviour when the bogie moves from the embankment to the bridge. At the moment, one wheel of the bogie is on the embankment and the other on the bridge, and more loads distribute to the wheel on the embankment due to its low position. As a result, the wheel–rail interaction force is increased in the zone corresponding to the wheel distance in a bogie (2.5 m/2.8 m). Following this hypothesis, the force of the rear wheel reaches the maximum when the bogie is half on the embankment and half on the bridge (1.25 m/1.4 m). This hypothesis is in agreement with the results of the numerical simulations of transition zones, where the higher ballast stresses were also observed on the distance depending on the wheel distance in a bogie.[4] It also explains the reason that the highest rail displacement appears at −0.9 or −1.5 m instead of −0.3 m, which is different from the bridge–embankment transition in Transition B (see 'Dynamic profiles of the embankment–bridge and bridge–embankment transitions' section).

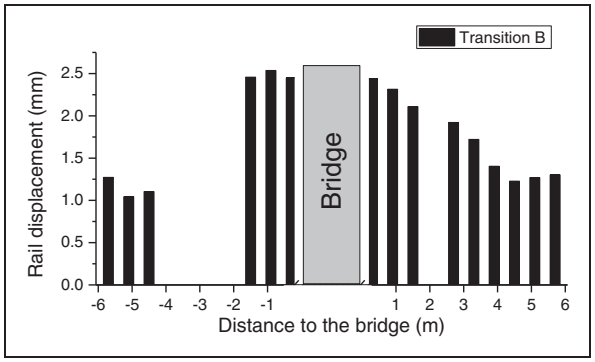

Figure 12. Statistics of the vertical rail displacements at all measured points of Transition B.

Discussion

From the measurement results presented above, it can be observed that the rail displacements in 0.3−1.5 m of Transition A were bigger than in Transition B, while the rail displacements in 4.5–5.7 m were very close. It matches very well with the maintenance history of these transitions (Transition A in poor condition and Transition B in good condition). It has been found the ratio of the average of the rail displacements in 0.3–1.5 m over those in 4.5–5.7 m has a correlation to the performance of the transition zones. The physical meaning of the ratio is how

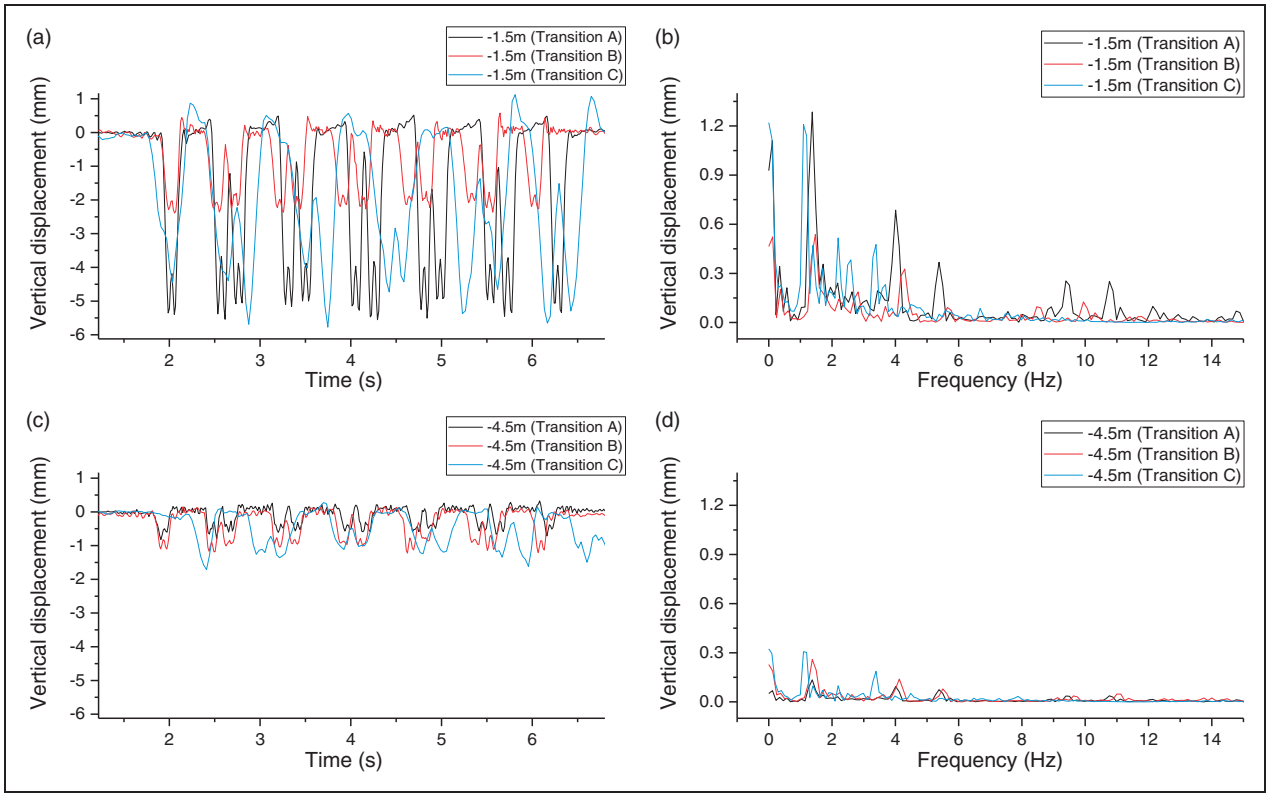

Figure 13. Rail vertical displacement of Transition B at −1.5 and −4.5 m compared with Transition A.

Table 4. Peaks (mm) corresponding to bogies in Figure 13.

	Transition A		Transition B		Transition C	
Bogie no.	−1.5 m	−4.5 m	−1.5 m	−4.5 m	−1.5 m	−4.5 m
1	5.39	0.82	2.39	1.11	4.45	1.71
2	5.54	0.80	2.36	1.19	4.40	1.26
3	5.08	0.60	2.27	1.01	5.69	1.36
4	5.16	0.61	2.36	1.04	4.02	1.11
5	5.00	0.56	2.27	0.96	5.77	1.03
6	5.27	0.57	2.20	0.96	4.73	1.24
7	5.55	0.59	2.26	1.02	4.43	1.20
8	5.51	0.59	2.14	1.22	5.37	1.34
9	4.94	0.49	2.23	0.86	4.65	1.62
10	5.05	0.56	2.08	0.96	5.65	1.49
11	5.45	0.66	2.36	1.14	5.29	1.15
12	5.34	0.72	2.26	1.21	3.84	1.08
Average	5.27	0.63	2.27	1.06	4.86	1.30
Standard deviation	0.21	0.10	0.09	0.11	0.64	0.21

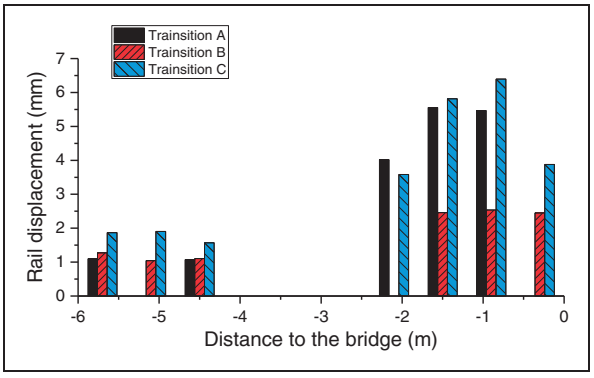

Figure 14. Comparison of vertical rail displacements in the approaching zone of two transitions.

many times larger the rail displacement is in the approaching zone than in the open track. The calculations are shown in Table 5, where $Rail_{0.3-1.5\,m}$ is the average of the rail displacement at 0.3–1.5 m; and $Rail_{4.5-5.7\,m}$ is the average of the rail displacement at 4.5–5.7 m. The distance is calculated from the bridge and only on the embankment–bridge transition as shown in Figure 7.

As seen in Table 5, the ratio correlates very well to the condition of the transition zones, wherein 2.2 is for the healthy condition and 5.1 for the poor condition. According to Kerr and Moroney,[1] Stark and Wilk[5] and Dahlberg,[39] the settlement in the transition zone is a self-perpetuating system. The differential settlement leads to redistribution of wheel load, which in turns initiates larger differential settlement. Assuming the ratio is 1 for a perfect transition zone, when no settlement exists in the approaching zone and $Rail_{0.3-1.5\,m}$ and $Rail_{4.5-5.7\,m}$ are same. As the transition is in use, the ratio increases. The higher value indicates the worse condition of the transition zone, while the lower value the healthier. Therefore, the ratio can reflect the degradation of a transition zone. By measuring the ratio of a transition zone, it is possible to know in which condition the transition is. For Transition C, both high $Rail_{0.3-1.5\,m}$ and $Rail_{4.5-5.7\,m}$ lead to a relative lower ratio, compared to Transition A. It indicates the open track is in poor condition as well as the approaching zone.

Table 5. Calculation of the measurements from the transition zones.

Transition	Condition	$Rail_{0.3-1.5\,m}$ (mm)	$Rail_{4.5-5.7\,m}$ (mm)	Ratio
A	Poor	5.51	1.08	5.1
B	Good	2.48	1.14	2.2
C	Poor	5.36	1.78	3.0

Since currently there is no special detection method or Key Performance Index (KPIs) for transition zones and maintenance scheme of transition zones are determined mostly by experience, this method has a potential to assess the condition and to determine maintenance scheme for certain types of transition zones. However, it should be noted that the ratio obtained here is for the transition zones without countermeasures with Dutch passenger trains running at normal operational velocity (80–140 km/h). These values may be affected by the transition zone type, configuration and velocity of trains. Before using the ratio as a KPI for transition zones, numerous measurements of transition zones should be conducted.

Conclusion

This paper presents the results of the experimental study performed on three transition zones in various conditions. The dynamic displacements of rails were measured at multiple points in the approaching zone. The measurement device employed is a contactless mobile device for measuring displacements, which is based on the DIC technique. Using this method, the dynamic profile of the track (the dynamic displacement of rail along the track) in the approaching zones (instead of a single point measurement) can be obtained. The health condition in the transition zones can be assessed, and therefore the maintenance schemes can be better determined.

Because the operational parameters of the DIC-based devices are important for accuracy, the measurement device was tested in the laboratory to determine the optimal range of its operational parameter. It has been found that the elevation angle of the cameras is the most sensitive parameter and a set of the operational parameter is proposed for the field measurement.

After determining the working ranges of the operational parameters, the measurements were performed on three transition zones. The length of the approaching zone (4.5 m) was determined based on the measurements performed at the different distances from the bridge. The rail displacements are considerably increased in the approaching zone, while the rail displacements are similar to those in the open track, beyond the approaching zone.

It has also been found that the dynamic profiles of the embankment–bridge and the bridge–embankment transition are both increased close to the bridge. However, the rail displacement in the embankment–bridge transition gradually decreases, while the highest rail displacement in the bridge–embankment transition appears at 0.9 or 1.5 m to the bridge. A possible explanation is that more loads distribute to the wheel on the embankment when the bogie moves from the embankment to the bridge.

Another finding is that the dynamic profiles of the transition zone in various conditions are significantly different. The ratio between the rail displacements in 0.3–1.5 and 4.5–5.7 m is calculated to study the degradation in the approaching zones. The results show that the ratio has good correlation with the health condition of the measured transition zones.

Acknowledgement

The authors would like to thank Dr Ivan Shevtsov (from ProRail), Professor Rolf Dollevoet (from TU Delft), Yuewei Ma (from TU Delft), Ruud van Bezooijen (from Id^2 BV) and Grégoire H. V. Lambert (from Id^2 BV) for the assistance during field measurements. The authors are very grateful to all the reviewers for their thorough reading of the manuscript and for their constructive comments.

Declaration of Conflicting Interests

The author(s) declared no potential conflicts of interest with respect to the research, authorship, and/or publication of this article.

Funding

The author(s) received no financial support for the research, authorship, and/or publication of this article.

References

1. Kerr AD and Moroney BE. Track transition problems and remedies. *Proc Am Railw Eng Assoc* 1993; 94: 25.
2. Zuada Coelho B. *Dynamics of railway transition zones in soft soils*. Doctoral dissertation, University of Porto, Porto, Portugal, 2011.
3. Nicks JE. *The bump at the end of the railway bridge*. Doctoral dissertation, Texas A&M University, College Station, TX, USA, 2009.
4. Wang H, Markine VL, Shevtsov IY, et al. Analysis of the dynamic behaviour of a railway track in transition zones with differential settlement. In: *2015 joint rail conference,* San Jose, California, USA, March 2015, p.7. New York, USA: ASME.
5. Stark TD and Wilk ST. Root cause of differential movement at bridge transition zones. *Proc IMechE, Part F: J Rail and Rapid Transit* 2016; 230(4): 1257–1269.
6. Hölscher P and Meijers P. *Literature study of knowledge and experience of transition zones*. Delft report no. 415990-0011, 2007. Delft, The Netherlands: GeoDelft.
7. Varandas JN, Hölscher P and Silva MAG. Dynamic behaviour of railway tracks on transitions zones. *Comput Struct* 2011; 89: 1468–1479.
8. Hyslip JP, Li D and McDaniel C. Railway bridge transition case study. In: *Eighth international conference (BCR2A'09) on bearing capacity of roads, railways and airfields*, Champaign, IL, USA, 29 June–2 July, 2009, pp. 1341–1348. London, UK: CRC Press.
9. Sasaoka C and Davis D. *Long term performance of track transition solutions in revenue service*. Technology Digest TD-05-036, Transportation Technology Center Inc, Association of American Railroads, Washington, D.C, USA, 2005.
10. Li D and Davis D. Transition of railroad bridge approaches. *J Geotech Geoenviron Eng ASCE* 2005; 131(11): 1392–1398.
11. Plotkin D and Davis D. *Bridge approaches and track stiffness*. Final Report, DOT/FRA/ORD-08-01, Federal Railroad Administration, Washington, D.C, USA, 2008.
12. Le Pen L, Watson G, Powrie W, et al. The behaviour of railway level crossings: insights through field monitoring. *Transp Geotech* 2014; 1: 201–213.
13. Gallage C, Dareeju B and Dhanasekar M. State-of-the-art: track degradation at bridge transitions. In: *Proceedings of the 4th international conference on structural engineering and construction management 2013*, Kandy, Gampola Road, Peradeniya, Sri Lanka, 2013, pp.40–52. Sri Lanka: Nethwin Printers (Pvt) Ltd.
14. Paixao A, Fortunato E and Calcada R. Design and construction of backfills for railway track transition

zones. *Proc IMechE, Part F: J Rail and Rapid Transit* 2013; 229: 58–70.
15. Coelho B, Hölscher P, Priest J, et al. An assessment of transition zone performance. *Proc IMechE, Part F: J Rail and Rapid Transit* 2011; 225: 129–139.
16. Wang H, Markine V and Shevtsov I. The analysis of degradation mechanism in track transition zones using 3D finite element model. In: *Proceedings of the second international conference on railway technology: research, development and maintenance* (ed J Pombo), Ajaccio, Corsica, France, 8–11 April 2014, paper no. 227. Stirlingshire: Civil-Comp Press. doi:10.4203/ccp.104.227.
17. Markine V, Wang H and Shevtsov I. Experimental analysis of the dynamic behaviour of a railway track in transition zones. In: *Proceedings of the ninth international conference on engineering computational technology* (eds P Iványi and BHV Topping), Naples, Italy, 2–5 September 2014, paper no. 3. Stirlingshire: Civil-Comp Press. doi:10.4203/ccp.105.3.
18. Bezin Y, Iwnicki SD, Evans G, et al. An investigation of sleeper voids using a flexible track model integrated with railway multi-body dynamics. *Proc IMechE, Part F: J Rail and Rapid Transit* 2009; 223: 597–607.
19. Lundqvist A and Dahlberg T. Load impact on railway track due to unsupported sleepers. *Proc IMechE, Part F: J Rail and Rapid Transit* 2005; 219: 67–77.
20. Pinto N, Ribeiro CA, Gabriel J, et al. Dynamic monitoring of railway track displacement using an optical system. *Proc IMechE, Part F: J Rail and Rapid Transit* 2013; 229: 280–290.
21. Paixão A, Fortunato E and Calçada R. Transition zones to railway bridges: track measurements and numerical modelling. *Eng Struct* 2014; 80: 435–443.
22. Paixão A, Alves Ribeiro C, Pinto N, et al. On the use of under sleeper pads in transition zones at railway underpasses: experimental field testing. *Struct Infrastruct Eng* 2014; 11: 112–128.
23. Macdonald J, Dagless E, Thomas B, et al. Dynamic measurements of the second Severn crossing. *Proc Instn Civil Engrs* 1997; 123(4): 241–248.
24. Koltsida I, Tomor A and Booth C. The use of digital image correlation technique for monitoring masonry arch bridges. In: *7th International Conference on Arch Bridges*, Split, Croatia, 2–4 October 2013, pp.681–690. Zagreb, Croatia: SECON-CSSE.
25. White D, Take W and Bolton M. Soil deformation measurement using particle image velocimetry (PIV) and photogrammetry. *Geotechnique* 2003; 53: 619–632.
26. McCormick N and Lord J. Digital image correlation for structural measurements. *Proc Instn Civil Engrs* 2012; 165: 185.
27. Murray C, Hoag A, Hoult NA, et al. Field monitoring of a bridge using digital image correlation. *Proc Instn Civil Engrs Bridge Eng* 2014; 168(1): 3–12.
28. Bhandari AR, Powrie W and Harkness RM. A digital image-based deformation measurement system for triaxial tests. *Geotech Test J* 2012; 35: 209–226.
29. Giachetti A. Matching techniques to compute image motion. *Image Vis Comput* 2000; 18: 247–260.
30. Tong W. An evaluation of digital image correlation criteria for strain mapping applications. *Strain* 2005; 41: 167–175.
31. Sutton M, Wolters W, Peters W, et al. Determination of displacements using an improved digital correlation method. *Image Vis Comput* 1983; 1: 133–139.
32. Bowness D, Lock A, Powrie W, et al. Monitoring the dynamic displacements of railway track. *Proc IMechE, Part F: J Rail and Rapid Transit* 2007; 221: 13–22.
33. Priest J, Powrie W, Yang L, et al. Measurements of transient ground movements below a ballasted railway line. *Géotechnique* 2010; 60: 667–677.
34. Priest JA and Powrie W. Determination of dynamic track modulus from measurement of track velocity during train passage. *J Geotech Geoenviron Eng* 2009; 135: 1732–1740.
35. Wheeler LN, Take WA and Hoult NA. Measurement of rail deflection on soft subgrades using DIC. *Proc Instn Civil Engrs Geotech Eng* 2016; 169: 383–398.
36. Ribeiro D, Calçada R, Ferreira J, et al. Non-contact measurement of the dynamic displacement of railway bridges using an advanced video-based system. *Eng Struct* 2014; 75: 164–180.
37. Murray CA, Take WA and Hoult NA. Measurement of vertical and longitudinal rail displacements using digital image correlation. *Can Geotech J* 2014; 52: 141–155.
38. Iryani L, Setiawan H, Dirgantara T, et al. Development of a railway track displacement monitoring by using digital image correlation technique. In: Xu Xipeng (ed) *Applied mechanics and materials*. Switzerland: Scitec Publications Ltd, 2014; 548, pp.683–687.
39. Dahlberg T. Railway track stiffness variations-consequences and countermeasures. *Int J Civil Eng* 2010; 8(1): 1–12.